

RAPID PROTOTYPED TERAHERTZ-DOMAIN GRADIENT INDEX OPTICS: COMPUTATIONAL DESIGN, SIMULATION, AND MANUFACTURE

Alexander Miles, William Duncan, Brian Klug, Colton Holmes

Faculty Sponsors: Dr. Hao Xin, Dr. Micheal Gehm
College of Optical Sciences, Department of Electrical and Computer
Engineering University of Arizona

ABSTRACT

There are a myriad of applications for terahertz radiation: security, military radar, product inspection, and telecommunications. These require manipulation of the radiation beyond simple transmission and detection, namely refraction: focusing, defocusing, and collimation.

The current state of the art fabrication of terahertz lenses is an expensive and time consuming processes; involving high purity semiconductors and months of lead time. Our project focused on demonstrating that an inexpensive and quick process could reduce the production investment required by more than three orders of magnitude. This process is based on fabrication using a novel gradient index structure produced with polymer-jetting rapid-prototyping machine.

1 INTRODUCTION

Optics that operate in the high gigahertz to terahertz ranges typically are inordinately expensive. This is due to the current state of manufacturing techniques that will be explained in 1.1. As a result, there is both large financial overhead, investment, and time required to go from tape out to physical realization and final construction. This project explores fabrication of similar EM spectrum domain structures using a polymer jetting technique which realizes much faster time of construction, and orders of magnitude less financial overhead. In addition, this project investigates the use of a gradient index (GRIN) structure to effect a lens. The same optical phenomena (focusing, defocusing, achromatizing) should be attainable from this gradient of index as one would expect from a optic with curved surfaces designed for a specific wavelength. The wavelengths this project is concerned with are on

the order of millimeters, meaning that the features that need be generated are substantially smaller than the wavelength. The interaction of the wave with these features can be modeled using effective medium theory, and give us very fine control of the index at each point, despite having relatively rough granularity over the the spatial distribution of material. The index profile was generated starting from an arbitrary four-parameter polynomial description, then optimized using a modified Levenberg-Marquardt algorithm. The resulting distribution was implemented using a dithered geometric distribution of two polymers available to be rapid-jet prototyped. Several physical designs for creating the index profile were created, and the simplest, a dithered combination of two polymers, was realized. Mapping indices to the physical geometrical distribution of material was achieved with an intermediate computation step and validation of the produced design was run in ANSYS HFSS, simulating the system response to an electromagnetic plane wave stimulus. HFSS simulates the full behavior by imposing specific boundary conditions upon Maxwell's equations, and therefore is a realistic interpretation of the actual performance expected from the geometries and indices simulated.

1.1 Existing Methods

The current state of manufacturing techniques for optics in the GHz to THz range is both time consuming and expensive, the most common technique is the traditional CMOS process utilized for semiconductor manufacturing which includes multiple several step processes from tape out of the design (optical mask) to exposure/photoresist development/acid etching to rinsing.

1.2 Effective Medium Theory

1.2.1 Introduction

Effective Medium Theory (EMT) provides for the mixing of different media based on general inclusion geometries in that their properties, usually and in our case electric permittivity ϵ is considered, can be effectively summed, averaged, or properly mixed (weighted) depending on application, inclusion geometry (cubical, spherical, ellipsoidal, etc.) and particular circumstance. Effective Medium Theory allows for the ability to mix different media, and predict the properties of the resulting material with respect to a certain feature size compared to the wavelength of concern.

1.2.2 Theory of Mixing

Mixing theory is based on the fact that essentially any volume (3D case) or area (2D case) that we wish to encapsulate and create a mathematical boundary therein can be found and material properties (in our case, electric permittivity) are known or can be found. The Maxwell-Garnett mixing formula [5]

$$\frac{\epsilon_{eff}}{\epsilon_e} = 1 + 3f \frac{\epsilon_i/\epsilon_e - 1}{\epsilon_i/\epsilon_e + 2 - f(\epsilon_i/\epsilon_e - 1)} \quad (1)$$

gives us a relation for implicitly finding the electric permittivity for a generic inclusion. In equation 1 above, ϵ_{eff} is the effective medium permittivity, ϵ_e is the permittivity of the

environment, in our case this is model polymer, ϵ_i is the permittivity of the inclusions, f is the dimensionless volume fraction of inclusions, in our case fraction of support to model polymers, in the effective medium. Based on the Maxwell-Garrent mixing formula the mixing of model and support polymer can be done successfully and implicitly.

2 METHODS AND ANALYSIS

2.1 Simulating Arbitrary Index Profiles

In order to simulate the index within the three-dimensional optic, we first made some simplifying assumptions. First, we assume that the resulting profile should be symmetric about the optical axis. Second, we assumed that the optic would be operating in air (with a nominal index of 1.0). This allowed us to simulate a single two dimensional slice, running from the optic axis to the edge, and the full depth of the optic with a small layer of air on the entrance side and a longer air buffer after the lens. This two-dimensional set of indices was stored as an array. No physical dimensions were imposed upon the model; only the aspect ratio of the device (aspects of 1 : 2, 1 : 3, and 1 : 4 were used during testing) was locked for each optimization.

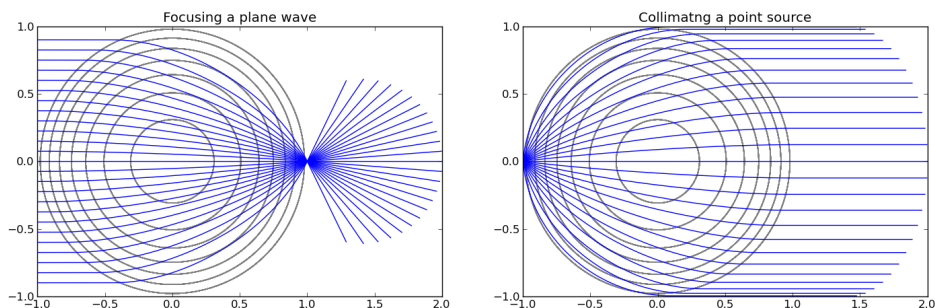


Figure 1: Raytracing simulation of a Luneberg lens index profile for validation of the raytracing algorithm. Black lines are contours of equal index of refraction, blue lines are traced rays.

2.2 Optimizing the Index Profile

A novel ray tracing algorithm was developed for determining ray paths through the distribution of index. This method requires a well-defined gradient of index, and in order to reduce the computational load of optimizing a totally arbitrary field, the index within the optic was constrained to those describable using the University of Rochester GRIN formula, seen below:

$$n(r, z) = n_{00} + n_{01}z + n_{02}z^2 + n_{03}z^3 + n_{04}z^4 + n_{10}r^2 + n_{20}r^4 + n_{30}r^6 + n_{40}r^8 \quad (2)$$

This allowed us to optimize utilizing only eight parameters, rather than allowing the optimizer to tweak the hundreds of thousands of elements within the array individually. It is important to note that being able to alter the individual elements in the physical optic is a great strength of rapid prototyping fabrication as compared to traditional methods of GRIN fabrication, but designing such a profile lay beyond the scope of our project. The optimization itself was done using a modified version of the Levenberg-Marquardt algorithm, which converges to stable local minimum even if the initial guess is very far away.

The figures of merit used during optimization were the standard deviation of the axial ray crossings (using between 25 and 100 rays), the difference between the desired axial crossing distance (typically the back focal distance, but in this case it remains unitless) from the optic and the average of the locations where the rays crossed. The final results of the optimization were the values of the eight coefficients, which were then used to generate an array of indices for the discretization process.

A proof of concept was undertaken to validate the function of the ray tracing algorithm. The test structure fed in was a Luneberg lens, a sphere with radially varying index of refraction. The index profile for this test structure can be modeled as follows, wherein r is the radial distance, R is the sphere radius, n_0 is the index of refraction of the surrounding medium, and n_1 is the highest index expected within the domain:

$$r = \sqrt{(x - x_c)^2 + (y - y_c)^2} \quad (3)$$

$$n(x, y) = \begin{cases} r \leq R & \sqrt{n_1 - \left(\frac{r}{R}\right)^2} \\ r > R & n_0 \end{cases} \quad (4)$$

The well-documented behavior of a Luneberg lens profile is to focus collimated light entering one side onto a focused spot on the opposite side, and take light from an object in contact with one side and emit collimated light out the opposite side. The result of tracing this profile can be seen in Figure 1 to follow this behavior exactly.

2.3 Discretization the Index Profile

The index profile optimization step yielded a continuously defined function that returns the index of refraction at any point in space. While convenient for a simulation, it was not convenient for fabricated. In order to affect the index at one given point, we fall back to the aforementioned effective medium theory, which holds that the material properties in a volume will act in concert as the volume-average material property. As such, we needed to find a scheme for distributing our three materials (model polymer with $n_{eff} = 1.7$, support polymer with $n_{eff} = 2.0$, and air $n_{eff} = 1.0$) in space that meshed well (no pun intended)

with the capabilities of the rapid prototyping machine available. Two specific schemes were settled upon as being realistic and computationally designable (as the complexity of the profile quickly went beyond what one would want to discretize by hand).

The first such scheme was dithering. In image processing this process takes an image possessing many intensity levels and, using a set of quantized intensity levels of our choice, re-builds the image using only the allowed intensity levels by propagating the difference between the quantized levels and the existing level to neighboring pixels. The result is an image that resembles the original when viewed at a different scale and lacks visible quantization steps that a straight threshold or halftone dither would result in. This is the same scheme utilized by comic book printers years ago to affect gradients with only discrete points of ink, as shown in Figure 2. We implemented a modified Floyd-Steinberg dithering algorithm and used it for discretization. This algorithm is commonly used in image processing and yields good uniformity and minimal quantization error over our average sizes. We also implemented an ordered dithering algorithm which turned out to be not as smooth and was thus abandoned, though the swiss cheese example later roughly approximates an ordered dither. Subjectively better smoothness was realized with the Floyd-Steinberg algorithm. Further experimentation with Bayer and other dither algorithms could potentially yield different, better results as well. This discretization algorithm was applied to each layer of the structure, in effect creating many area dithers rather than a true volume dither.

The second discretization scheme is nicknamed ‘swiss cheese’ since it approximates the holey structure of the cheese which it derives its namesake from. Simply put, the swiss cheese model consists of columns of one material surrounded by another material. One structure consisting of air surrounded by model polymer was designed, another consisting of support polymer surrounded by model polymer. In the swiss cheese system, the index varies only in x and y , not z through the optic. A two-dimensional slice of material is divided up into a regular grid. Each entry in the grid is replaced with a predefined structure whose volume average is closest to the desired index.

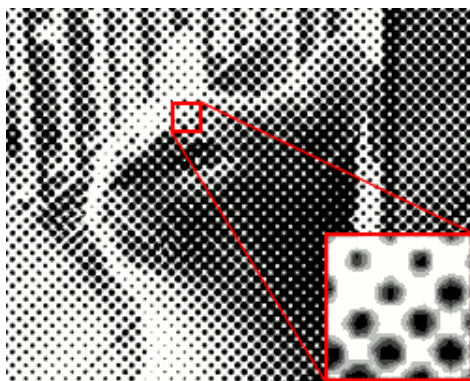


Figure 2: An example of how a “halftone” or dithered pattern effects a gradient on different length scales

2.4 EM Simulation

One avenue used to prove the focusing ability of our swiss cheese structure was simulating the structure in ANSYS HFSS. The HFSS software allowed for the structures to be built in three dimensions and simulated to observe electromagnetic plane wave behavior through and beyond our discretized structure. As will be discussed later, due to computational complexity and processing limitations not all of our designs were able to be simulated using HFSS, the dithered structure being one of these. The dithered model had on the order of one million more boundary conditions than the swiss cheese structure. However, the swiss cheese design was simulated to show, in simulation, that the focusing of a terahertz domain plane wave is possible with this structure.

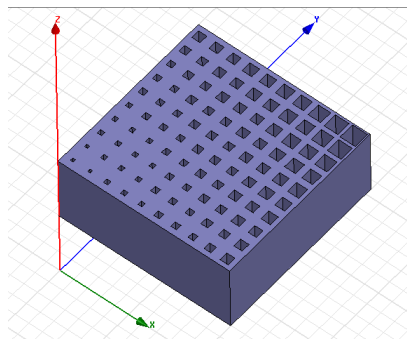


Figure 3: HFSS Model of the Swiss cheese discretization scheme

To simulate the design using HFSS the structure was built by hand using HFSS's built-in three dimensional model building features. Once built, individual portions of the structure was selected and assigned material properties, in particular the dielectric constant for relevant regions was set to those of the model and support polymers. Other methods were considered but not implemented in building the structures for simulation. The first involved building the structures using the SolidWorks three dimensional model building software, which allows for greater design detail, and importing the structure into HFSS using a .STEP file extension. This seemed to be illogical because our structures were able to be built with similar precision and difficulty using HFSS which excludes the process of transferring the simulated structure between different software. The second method considered was creating script files generated using MATLAB in order for the structures to be built automatically. This method would have been useful in order to build the dithered solid block design in HFSS because of the complexity of the structure. However, because of foreseen computational limitations, the dithered model was not attempted to be simulated using HFSS. Thus, work in generating the script files was not undertaken.

Due to high radial symmetry and no z -directional variation in index profile it was possible to build only a quarter of the structure in HFSS to reduce computation time while still obtaining significant results. A radiation boundary was built around the structure and extended out to an appropriate distance where the focal point was predicted to fall inside, in general about five times the depth of the structure. An incident plane wave within the tera-

hertz frequency region was selected to travel normal to the surface of the selected entry plane of the structure. Further, observation planes (ones with unassigned material properties, and therefore air) were placed at stepped z -varying distances in order to observe electromagnetic intensity activity as the plane wave travels through and beyond the structure. The simulations were then analyzed by the HFSS software which took between 20 minutes to multiple hours depending on the complexity.

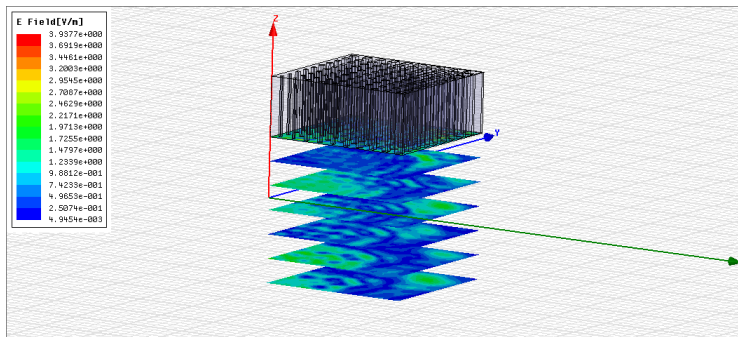


Figure 4: HFSS Results near the focal plane

Focusing effects were observed in HFSS simulation of the Swiss Cheese dithered design as seen in Figure 3. Again, only a quarter of the entire structure was built to decrease computation/processing time. The dimensions of the optics are (2.5 cm x 2.5 cm x 1 cm) in $(x y z)$. The original design called for a depth in z of 2 cm although when simulated an “out of memory” error occurred on the computer so the structure depth was cut in half so computation was possible. The incident plane wave tested on the structure was set at 100 GHz which translates to a 3 mm wavelength. By cutting the depth of the structure in half the incident wave was still able to pass the distance of just over three wavelengths through the material. It is untested as to whether having a thicker depth would provide better or worse focusing effects. Although it would decrease the intensity of the plane wave due to absorption and reflection effects by the structure. It is known that both the model and support polymers are quite optically dense. From this simulation the results show the best focusing desired at 2 mm and 8 mm from the exiting surface of the swiss cheese structure. The multiple peaks of intensity suggest a less focused result than a well defined focal point which is a result of having a lack of z - varying index. However it does show that focusing is possible with the use of varying polymer materials at sub-wavelength increments which can be understood through effective medium theory. Figure 5 is a visual representation of the intensity of the plane wave focused at where the center of the structure would be if the whole structure was simulated.

3 RESULTS AND DISCUSSION

Testing of the current optics is being done with a Fourier transform spectrometer and has been more time consuming than expected. As a result, testing is still underway and data is

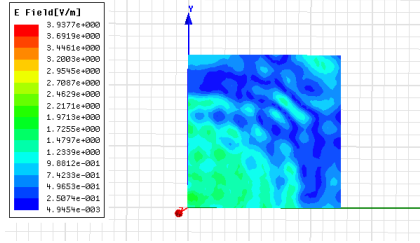


Figure 5: HFSS Results near the focal plane

still being collected. The team is confident that these data will be meaningful. Acquiring a source capable of producing 300 GHz was one of the major challenges that needed to be overcome. There has been a concern that the optics, as produced currently, will cause too much loss of the electromagnetic field. Should the loss show to be overwhelming, the optics can simply be scaled to a smaller, thinner structure while keeping the aspect ratio of height to thickness constant at a minor cost of production and time, exactly one of the benefits of this fabrication method.

4 CONCLUSIONS

It has been readily shown here that through the use of a rapid prototyping polymer jetting machine structures can be produced that can effect terahertz domain waves. The benefit of using a rapid prototyping polymer jetting machine has also been shown to reduce both fabrication cost and time several orders of magnitude with respect to the current industry standard, semiconductor processing. As a proof of concept project, this means of production for terahertz optics has been a success and shows great promise.

5 ACKNOWLEDGMENTS

We'd like to thank Dr. Hao Xin and Dr. Michael Gehm for use of the Objet EDEN 350 Rapid Prototyping Machine as well as for experimental guidance.

References

- [1] M.E. Gehm, Z. Wu, and H. Xin. Rapid prototyping for fabrication of GHz-THz bandgap structures (Proceedings Paper). 2009.
- [2] E. Hecht. Hecht optics, 1998.
- [3] W.R. Ng, A. Pyzdek, Z. Wu, H. Xin, and M.E. Gehm. Computer-Generated Volume Holograms in the THz. In *Frontiers in Optics*. Optical Society of America, 2010.
- [4] W.R. Ng, Z. Wu, H. Xin, and M.E. Gehm. Fabrication of GHz/THz Volumetric Optics via Rapid Prototyping. In *Frontiers in Optics*. Optical Society of America, 2009.

- [5] AH Sihvola. *Electromagnetic mixing formulas and applications*. Inspec/Iee, 1999.
- [6] Z. Wu, J. Kinast, ME Gehm, and H. Xin. Rapid and inexpensive fabrication of terahertz electromagnetic bandgap structures. *Optics Lett*, 16(21):16442–16451, 2008.
- [7] Z. Wu, W.R. Ng, M.E. Gehm, and H. Xin. Terahertz electromagnetic crystal waveguide fabricated by polymer jetting rapid prototyping. *Optics Express*, 19(5):3962–3972, 2011.